ACS Macro Letters

Letter

pubs.acs.org/macroletters

# Functionality- and Size-Dependent Target-Differentiation of Nanoporous Carboxylated Polystyrenes in Polar Protic Solvents

Jie Song and Byoung-Ki Cho*

Department of Chemistry and Institute of Nanosensor and Biotechnology, Dankook University, Gyeonggi-Do, 448-701, Republic of Korea

Supporting Information

**ABSTRACT:** In this study, we investigated the functionality- and size-dependent differentiation capability of bulk nanoporous polystyrene (PS) materials in aqueous environments. A three-arm star block copolymer (consisting of dibranched PS and linear polylactide (PLA) blocks) was employed to prepare PS nanochannels with the average pore diameter of 14.2 nm. Due to the ester group at the junction of the PS and PLA blocks, a negatively charged carboxylate group could be placed as the wall functional group automatically after the PLA etching. Based on specific electrostatic interactions, the bulk PS channels with the carboxylated wall could selectively capture a water-soluble cationic dye (rhodamine 6G) in the aqueous and methanolic solutions. Furthermore, the well-defined porous PS displayed excellent size-dependent selectivity, which was proved by a fluorescence quenching experiment using differently sized gold nanoparticles (AuNPs). Rhodamine 6G dyes on the pore wall were effectively quenched by 2 nm AuNPs. In contrast, the 16 nm AuNPs (larger than the pore diameter) did not affect the brightness of the rhodamine 6G-loaded PS.

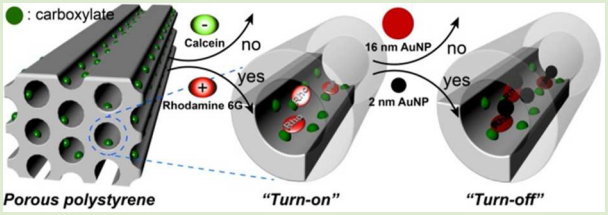


Molecular recognition in nanopores is an intriguing subject because of its tremendous application potential for separations, and sensors.[1] To enhance the selective capture in nanopores, two major factors (i.e., wall functionality and pore size) have to be optimized for a target analyte. Nanoporous polycarbonate (PC) membranes have been used as materials for chemical separations.[2] Several methods have been employed to control pore size and wall functionality. For example, electroless gold plating can tune the pore size by thickening the gold layer, and functional groups on the gold surface were modified by subsequent thiol treatment.[3] Moreover, charged polymers and dendrimers have been coated on the oppositely charged pore surface, thus, enabling both pore size and functionality to be controlled in a single step.[4] Although nanoporous PCs are beneficial in terms of pore control, they have low pore densities ($\sim 10^9$ pores/cm$^2$), and the pores are randomly distributed across the membranes.[5]

The self-assembly of block copolymers (BCPs) consisting of chemically inert and labile blocks can provide an alternative way to prepare nanoporous polymers.[6] In contrast to PC membranes, the nanopores from BCP assemblies are regularly arrayed, and the pore densities are as high as $10^{11}$ pores/cm$^2$.[7]

Although other block copolymer samples (e.g., polybutadiene-*block*-polydimethylsiloxane) were employed,[8] polystyrene-*block*-polylactide (PS-*b*-PLA) is a representative polymer precursor for the preparation of nanoporous polymers, which has been intensively studied by the Hillmyer group.[7,9] Some results regarding the postmodification of wall functionalities and thin film applications have been reported.[10] Nevertheless, except for a capsule-like PS tube with a single pore recently reported to discriminate charged analytes,[11] no bulk PS with a regular array of nanopores has been applied to molecular separations.

Therefore, it is worth investigating separation events in organic nanopores coming from designed BCPs. To do so, we employed a three-arm star $(PS)_2$-*b*-PLA with its PS volume fraction ($f$) of 0.6 (Figure 1a). The three-arm star architecture was chosen to obtain a hexagonal columnar morphology with PLA cylindrical cores, because the branched block makes the curvature toward the linear block in order to relieve some packing constraints.[12] According to the theoretical studies of miktoarm block copolymer assemblies, the relaxation of the multiarm block favors the outside of the curved interface at the expense of a gained stretching energy of the inner linear block.[13] Indeed, the three-arm star block copolymer showed a hexagonal columnar morphology (Figure 1b and Figure S1(a)), while the linear PS-*b*-PLA with the identical $f$ exhibited a lamellar morphology.[14] In the BCP design, it should also be noted that a removable ester group was placed at the junction of the PS and PLA blocks (Figure 1a). Thus, it automatically changed into a negatively charged carboxylate on the PS wall by a NaOH etching step (Figure 1c).

The three-arm block copolymer was prepared by a click reaction of dibranched PS and PLA blocks (Scheme S1).[15] The obtained star block copolymer could be converted into well-defined monolithic nanoporous PS (**1**) with the average pore diameter of 14.2 nm (Figure S2). Assuming that all the

**Received:** October 4, 2012
**Accepted:** November 13, 2012
**Published:** November 16, 2012

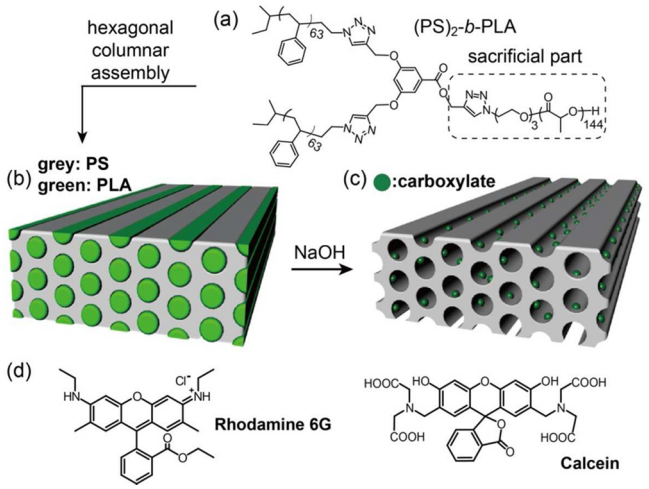


**Figure 1.** (a) Molecular structure of $(PS)_2$-*b*-PLA, and schematic representations of (b) the hexagonal columnar structure assembled by $(PS)_2$-*b*-PLA and (c) the nanoporous PS (**1**) after removing the PLA block using NaOH. (d) Molecular structures of rhodamine 6G and calcein.

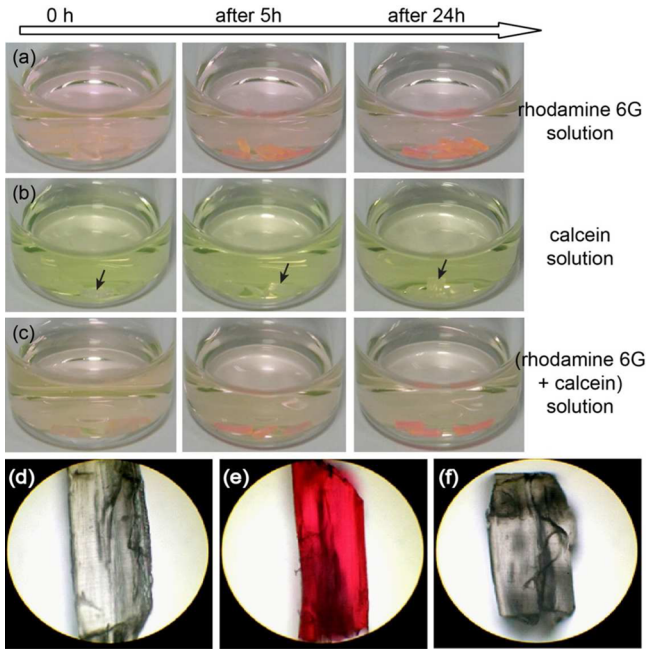


**Figure 2.** Time-dependent photographs of the porous PS pieces in methanolic (a) rhodamine 6G, (b) calcein, and (c) rhodamine 6G/calcein mixture solutions. (d–f) Bright field micrographs (10×). (d) Pristin porous PS (**1**). (e, f) Solvent-free porous pieces taken from methanolic rhodamine 6G and calcein solutions, respectively. In (b), PS pieces at the bottom are indicated by the arrows.

carboxylate groups were placed on the surface, the areal density of the carboxylate functional groups was estimated to be 0.33/nm$^2$ using the specific surface area (determined from the nitrogen sorption experiment) and molecular weight of the PS block. The experimental method, including macroscopic orientation and chemical etching processes, was performed as similar to what the Hillmyer group reported previously. The regarding experimental details including the porosity characterizations are presented in Supporting Information.

As confirmed by the $^1$H NMR and gel permeation chromatography (GPC) results (Figure S4), the PLA block was completely removed by a chemical etching using NaOH solution. Therefore, anionic carboxylate groups were placed on the pore wall (Figure 1c). With this in mind, we considered that the PS nanochannels with the negatively charged walls could capture positively charged analytes that are small enough to penetrate into porous channels. To demonstrate this hypothesis, we examined the electrostatics-based differentiation of **1**. We chose two water-soluble dyes (i.e., rhodamine 6G and calcein) as the analytes, because they are analogous in size and structure, but different in charge (Figure 1d). With the naked eye, the dye differentiation of **1** was preliminarily examined in the methanolic solutions containing rhodamine 6G and calcein, respectively. The PS pieces in the rhodamine 6G solution turned pink, while no color was observed in the calcein solution (Figure 2a,b). In addition, the color in the mixture solution of the two dyes was seemingly identical to that in the rhodamine 6G solution (Figure 2c). The direct observation of the PS pieces taken from the dye solutions using an optical microscope was identical to the above observation. The entire area of the solvent-free PS sample from the rhodamine 6G solution turned red, while the sample from the calcein solution looked translucent gray (the same as the pristine PS (**1**); Figure 2d–f).

More elaborate experiments were performed in the aqueous solutions because our porous PS is potentially applied to biological targets such as water-soluble proteins.[16] Because the density of **1** is lower than water, the porous PS pieces were sealed in aluminum foil with holes and then immersed in the 10 $\mu$M aqueous solutions of rhodamine 6G and calcein. As the amount of **1** added increased, we checked the dye concentrations in the solutions. As with the observation in the methanolic solutions, it was noticeable with the naked eye that the rhodamine 6G solution became lighter than the calcein solution with increasing amounts of porous PS (Figure 3a,b). The quantitative analysis was done by monitoring the UV–vis absorption data of the solutions. The absorbance of the rhodamine 6G solution decreased from 0.63 to 0.51 and 0.23 with increasing amounts of **1** (Figure 3a), because the rhodamine 6G molecules in the solution diminished due to the insoluble porous PS sieving rhodamine 6G molecules (Figure 3f). In contrast, only a tiny absorbance reduction was observed in the calcein solution, although identical amounts of **1** were added (Figure 3b).

Besides the spectroscopic evidence, it is necessary to verify the permeation of the dye molecules into PS pores. First, we investigated a nonporous PS homopolymer with a carboxylic acid group (see Scheme S1). The nonporous PS was immersed in the aqueous rhodamine 6G solution. In contrast to the PS sample (**1-Rho**) taken from the rhodamine 6G solution, the nonporous sample did not turn red (Figure S7). This suggests that the red porous PS in the rhodamine 6G solution comes not from the exterior surface, but from the interior pore area.

To investigate this in more detail, we examined the fluorescence microscope images of **1**, **1-Rho**, and **1-Cal** (taken from the calcein solution). The samples were excited at 510 nm. No emissive region was observed in the fluorescence image of **1**. For **1-Rho**, a strong emission was observed over the whole sample area, which also indicates that cationic molecules permeated into the internal pores of the sample (Figure 3f). In contrast, **1-Cal** was less bright, and slightly emissive regions were found near the sample edge. This means that calcein molecules could not penetrate into internal pores but were slightly loaded in pores at the edge areas (Figure 3g).


dx.doi.org/10.1021/mz3005154 | *ACS Macro Lett.* 2012, 1, 1375–1378

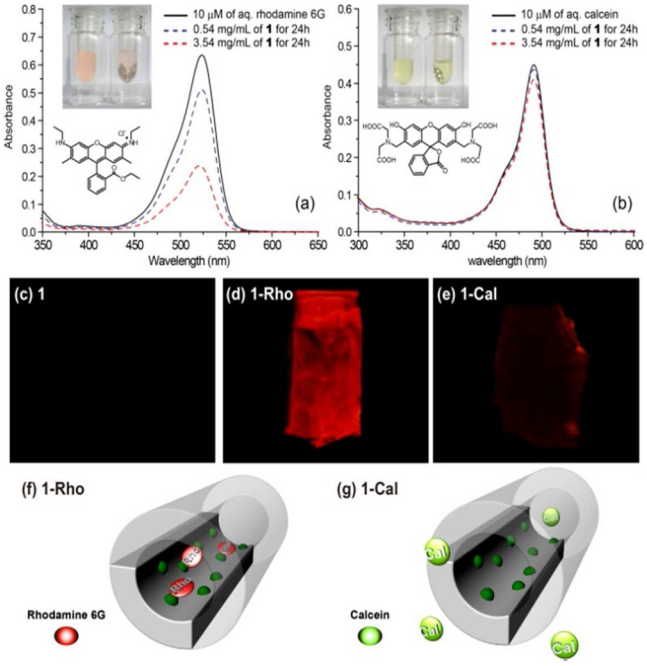


**Figure 3.** UV−vis absorption variations of (a) rhodamine 6G solution and (b) calcein solution as a function of the amount of **1** added. In the vial photos, the left and right images were taken before and after the addition of **1**. (c−e) Fluorescence microscope images and (f, g) schematic representations: (c) **1**, (d, f) the PS sample (**1-Rho**) taken from the rhodamine solution, and (e, g) the PS sample (**1-Cal**) taken from the calcein solution.

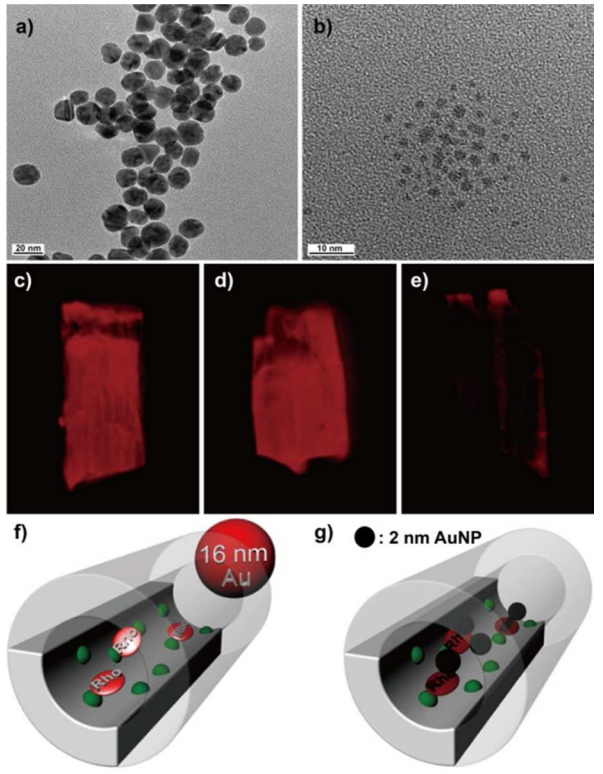


**Figure 4.** Transmission electron micrographs of (a) 16 nm AuNP and (b) 2 nm AuNP. Fluorescence microscope images (c−e) and schematic representations (f, g): (c) **1-Rho**, (d, f) **1-Rho** immersed in 16 nm AuNP solution, and (e, g) **1-Rho** immersed in 2 nm AuNP solution.

The above experimental results demonstrate **1** can recognize selectively cationic analytes via the electrostatic interaction of anionic carboxylate groups on the wall. Consequently, pore functionality is an important parameter for molecular discrimination.

Meanwhile, gold nanoparticles (AuNP) are frequently employed as a quencher for many dye molecules. It is well-known that rhodamine 6G is quenched by AuNPs of various sizes.[17] With this in mind, we envisaged that AuNPs with different diameters could prove the size-dependent recognition in porous PS materials. To test this, we prepared two AuNPs with average diameters of 2 and 16 nm, respectively (Figures 4a,b and S8). The surface groups of the AuNPs were carboxylic acid. Taking into account the sparse population (0.33/nm$^2$) of the carboxylate group of **1** and the molecular area (1.85 nm$^2$)[18] of rhodamine 6G, the rhodamine 6G in **1-Rho** presumably can only interact with one carboxylate group on the wall. Therefore, the remaining nitrogen moiety of rhodamine 6G has the possibility to interacts with carboxylic acid units on the AuNP surface. Because both AuNPs had the identical acid functionality, the surface effect for quenching rhodamine 6G could be ruled out. Therefore, we assumed that the dye quenching was mainly attributed to the different AuNP diameters relative to the PS pore diameter. The concentrations of the 2 and 16 nm AuNP solutions were determined to be 10 $\mu$M and 56 nM, respectively. The rhodamine 6G-containing PS sample (**1-Rho**) was immersed in each AuNP solution. After a prolonged immersion of 4 days, the PS samples were investigated using fluorescence microscopy. The samples were excited at 510 nm. The PS sample taken from the 16 nm AuNP solution was as bright as **1-Rho** before immersion in the AuNP solution (Figure 4c,d). This suggests that 16 nm AuNPs cannot interpenetrate the nanopores of **1-Rho**, because the particle diameter is larger than the pore diameter (Figure 4f). In contrast, the PS sample from the 2 nm AuNP solution became dimer than **1-Rho** (Figure 4e). This indicates that 2 nm AuNPs permeated nanopores and effectively quenched rhodamine 6G dyes in the pore interior (Figure 4g). Consequently, the results clearly demonstrate the influence of particle size on dye fluorescence in nanopores.

In summary, we have verified that the porous PS (**1**) can be utilized as a polymeric sieve for nanosized analytes. Because of the controlled wall functionality (anionic carboxylate), **1** was able to selectively capture positively charged rhodamine 6G. In addition, **1** with the 14.2 nm pore diameter exhibited excellent size-dependent selectivity. The 2 nm AuNPs effectively quenched rhodamine 6G on the porous wall, while the 16 nm AuNPs did not affect the brightness of the rhodamine 6G-loaded PS. We believe that the nanoporous PS can be diversely applied for the development of smart chromatographic materials for nanosized chemical and biological analytes.

## ■ ASSOCIATED CONTENT

### Ⓢ Supporting Information

Experimental details, DSC, $^1$H NMR, SAXS, SEM, $N_2$ adsorption−desorption curves, optical micrograph, and gold-nanoparticle size distribution data. This material is available free of charge via the Internet at http://pubs.acs.org.

## ■ AUTHOR INFORMATION

### Corresponding Author

*E-mail: chobk@dankook.ac.kr.

## Notes

The authors declare no competing financial interest.

## ■ ACKNOWLEDGMENTS

This work was supported by the National Research Foundation (NRF) of Korea grant funded by the Ministry of Education, Science and Technology (MEST), Republic of Korea (Nos. 2009-0084501 and 2012R1A2A2A01045017).

## ■ REFERENCES

(1) (a) Lee, S. B.; Mitchell, D. T.; Trofin, L.; Nevanen, T. K.; Söderlund, H.; Martin, C. R. *Science* **2002**, *296*, 2198. (b) Wiesenauer, B. R.; Gin, D. L. *Polym. J.* **2012**, *44*, 461.

(2) Jirage, K. B.; Hulteen, J. C.; Martin, C. R. *Science* **1997**, *278*, 655.

(3) (a) Jirage, K. B.; Hulteen, J. C.; Martin, C. R. *Anal. Chem.* **1999**, *71*, 4913. (b) Wirtz, M.; Yu, S.; Martin, C. R. *Analyst* **2002**, *127*, 871. (c) Yu, S.; Lee, S. B.; Kang, M.; Martin, C. R. *Nano Lett.* **2001**, *1*, 495.

(4) (a) Savariar, E. N.; Krishnamoorthy, K.; Thayumanavan, S. *Nat. Nanotechnol.* **2008**, *3*, 112. (b) Savariar, E. N.; Sochat, M. M.; Klaikherd, A.; Thayumanavan, S. *Angew. Chem., Int. Ed.* **2009**, *48*, 110.

(5) Martin, C. R. *Acc. Chem. Res.* **1995**, *28*, 61.

(6) (a) Olson, D. A.; Chen, L.; Hillmyer, M. A. *Chem. Mater.* **2008**, *20*, 869. (b) Uehara, H.; Yoshida, T.; Kakiage, M.; Yamanobe, T.; Komoto, T.; Nomura, K.; Nakajima, K.; Matsuda, M. *Macromolecules* **2006**, *39*, 3971. (c) Mao, H.; Hillmyer, M. A. *Macromolecules* **2005**, *38*, 4038. (d) Bolton, J.; Bailey, T. S.; Rzayev, J. *Nano Lett.* **2011**, *11*, 998. (e) Huang, K.; Rzayev, J. *J. Am. Chem. Soc.* **2009**, *131*, 6880. (f) Ho, R.-M.; Chen, C.-K.; Chiang, Y.-W.; Ko, B.-T.; Lin, C.-C. *Adv. Mater.* **2006**, *18*, 2355.

(7) Zalusky, A. S.; Olayo-Valles, R.; Taylor, C. J.; Hillmyer, M. A. *J. Am. Chem. Soc.* **2001**, *123*, 1519.

(8) (a) Li, L.; Schulte, L.; Clausen, L. D.; Hansen, K. M.; Jonsson, G. E.; Ndoni, S. *ACS Nano* **2011**, *5*, 7754. (b) Berthold, A.; Sagar, K.; Ndoni, S. *Macromol. Rapid Commun.* **2011**, *32*, 1259.

(9) (a) Zalusky, A. S.; Olayo-Valles, R.; Wolf, J. H.; Taylor, C. J.; Hillmyer, M. A. *J. Am. Chem. Soc.* **2002**, *124*, 12761. (b) Gorzolnik, B.; Daivdson, P.; Beurroies, I.; Denoyel, R.; Grande, D. *Macromol. Symp.* **2010**, *287*, 127.

(10) (a) Rzayev, J.; Hillmyer, M. A. *Macromolecules* **2005**, *38*, 3. (b) Rzayev, J.; Hillmyer, M. A. *J. Am. Chem. Soc.* **2005**, *127*, 13373.

(11) Huang, K.; Rzayev, J. *J. Am. Chem. Soc.* **2011**, *133*, 16726.

(12) (a) Cho, B.-K.; Jain, A.; Gruner, S. M.; Wiesner, U. *Science* **2004**, *305*, 1598. (b) Cho, B.-K.; Jain, A.; Gruner, S. M.; Wiesner, U. *Chem. Commun.* **2005**, 2143. (c) Chung, Y.-W.; Lee, J.-K.; Zin, W.-C.; Cho, B.-K. *J. Am. Chem. Soc.* **2008**, *130*, 7139. (d) Song, J.; Cho, B.-K. *Soft Matter* **2012**, *8*, 3419.

(13) (a) Pickett, G. T. *Macromolecules* **2002**, *35*, 1896. (b) Grason, G. M.; Kamien, R. D. *Macromolecules* **2004**, *37*, 7371.

(14) Song, J.; Cho, B.-K. *Bull. Korean Chem. Soc.* **2012**, in press.

(15) Ha, J.-G.; Song, J.; Lee, J.-K.; Cho, B.-K.; Zin, W.-C. *Chem. Commun.* **2012**, *48*, 3418.

(16) Park, M.-H.; Subramani, C.; Rana, S.; Rotello, V. M. *Adv. Mater.* **2012**, *24*, 5862.

(17) (a) Saha, D.; Agasti, S. S.; Kim, C.; Li, X.; Rotello, V. M. *Chem. Rev.* **2012**, *112*, 2739. (b) Dulkeith, E.; Morteani, A. C.; Niedereichholz, T.; Klar, T. A.; Feldmann, J.; Levi, S. A.; van Veggel, F. C. J. M.; Reinhoudt, D. N.; Möller, M.; Gittins, D. I. *Phys. Rev. Lett.* **2002**, *89*, 203002.

(18) The molecular area of rhodamine 6G was obtained by dividing the molecular volume (0.63 $nm^3$) by the molecular thickness (0.34 nm).